World Academy of Science, Engineering and Technology
International Journal of Mechanical and Mechatronics Engineering
Vol:9, No:5, 2015

Modeling and Validation of Microspheres Generation in the Modified T-Junction Device

Lei Lei, Hongbo Zhang, Donald J. Bergstrom, Bing Zhang, K. Y. Song, W. J. Zhang

***Abstract*—**This paper presents a model for a modified T-junction device for microspheres generation. The numerical model is developed using a commercial software package: COMSOL Multiphysics. In order to test the accuracy of the numerical model, multiple variables, such as the flow rate of cross-flow, fluid properties, structure, and geometry of the microdevice are applied. The results from the model are compared with the experimental results in the diameter of the microsphere generated. The comparison shows a good agreement. Therefore the model is useful in further optimization of the device and feedback control of microsphere generation if any.

***Keywords*—**CFD modeling, validation, microsphere generation, modified T-junction.

I. Introduction

MICROSPHERES have many important applications: drug delivery system (DDS), cosmetics, food, and other industrial uses. For the recent decades, microsphere produced with microfluidic technology has gathered a tremendous attention, such as T-junction [1]-[10], membrane emulsification [11]-[13], and flow focusing [14], [15]. In the original T-junction approach, the size of middle flow is determined by the size of the microchannel, and this means that the size of microspheres could only be adjusted in a very small range. To overcome this disadvantage, a modified T-junction device was developed by Song in 2011 in our group [16], as shown in Fig. 1. By introducing the sheath flow, the size of the middle flow is not only contributed by the size of microchannel but also the sheath flow rate. In this way, a tremendous economic value as well as the need of recycling the device has been achieved.

Although it has been proved that the controllability and uniformity of the microspheres generated using this device is acceptable [16], how the flow rate, channel size, and fluid property may influence the microspheres generation process has not been understood very well. Primary work has been done to study the effects from capillary number on the droplet formation in an analytical manner [17]. However, this model only considers part of the device structure.

The model in this paper considered the complete structure of the modified T-junction device. And this model could be further used for optimization and control the microsphere generation. Experiments were conducted to validate the model.

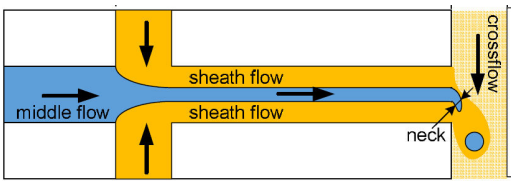

Fig. 1 Schematic diagram of a modified T-junction device: Three flows are involved: middle-flow, sheath-flow, and cross-flow. The fluid of sheath-flow and corss-flow are the same, which is immiscible with middle-flow [16]

II. Materials and Properties

In this work, Poly(lactic-co-glycolic acid) (PLGA) dissolved in dichloromethane (DCM) with concentration of 1%, 5%, and 15%, respectively, were used as dispersed phase. Polyvinyl alcohol (PVA) dissolved in distilled water with concentration of 1% was used as continuous phase. The physical properties are listed in Table I.

TABLE I
Physical Properties of Fluids

	Concentration (%)	Density (g/cm^3)	Viscosity (Pa.s)
PLGA	1	1.329	0.12
	5	1.326	0.19
	15	1.315	0.33
PVA	1	1	1.702 [18]

PLGA (50/50, inherent viscosity 0.16-0.24 dl/g) was purchased from Jinan Daigang Biomaterial Co., Ltd (Jinan, Shandong, China), and Evonik Industries AG (Essen, Germany). PVA (Mw 85,000-124,000, 99+% hydrolyzed) was purchased from Shanghai Lingfeng Chemical Reagent Co., Ltd (Shanghai, China). DCM was purchased from Shanghai Chemical Reagent Co., Ltd (Shanghai, China). PDMS microchannel was fabricated in Shanghai Wenchang Chip Technology Co., Ltd (Shanghai, China).

III. Structure of the Device

There were two structures of the modified T-Junction in this study: modified T-junction with straight channel, and modified T-junction with crooked channel, as shown in Fig 2 (a) and (b),

Lei Lei, Hongbo Zhang is with East China University of Science and Technology, Shanghai, 200237 China (e-mail: leileiearth@gmail.com, hbzhang@ecust.edu.cn).
Donald J. Bergstrom is with the Mechanical Engineering Department, University of Saskatchewan, Saskatoon, SK S7N5A9 Canada (e-mail: don.bergstrom@usask.ca).
Bing Zhang is with the Biomedical Engineering Division, University of Saskatchewan, Saskatoon, SK S7N5A9 Canada (e-mail: 080506zb@gmail.com).
Ki Young Song is with the East China University of Science and Technology, Shanghai, 200237 China and Biomedical Engineering Division, University of Saskatchewan, Saskatoon, SK S7N5A9 Canada (email: sky8071@gmail.com)
Wenjun Zhang is with the Mechanical Engineering Department and Biomedical Engineering Division, University of Saskatchewan, Saskatoon, SK S7N5A9 Canada (e-mail: chris.zhang@usask.ca).

respectively. For both structures, all the channels were uniform in width and height. The details of the devices are listed in Table II.

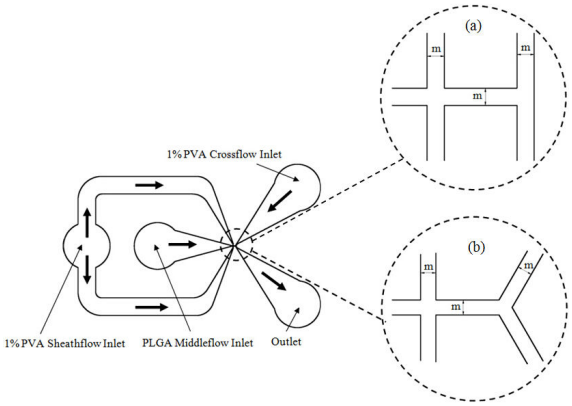

Fig 2 Schematic diagram of modified T-junction device: Channels are molded in PDMS. PLGA solutions with different concentrations are used: 1%, 5%, and 15%. m: channel width and height. (a) straight channel; (b) crooked channel

TABLE II
STRUCTURE AND DIMENSIONS OF MODIFIED DEVICE

Device	Structure	m (μm)
1	straight	50
2	straight	75
3	crooked	50
4	crooked	100

IV. The Model of the Droplet Formation Process

A. Governing Equation

The Level Set (LS) method [19] was used in this study, which represents the front profile of the droplet. The LS equation could be expressed as

$$\frac{\partial \phi}{\partial t} + \mathbf{u} \cdot \nabla \phi = \gamma \nabla \cdot \left[\varepsilon \nabla \phi - \phi(1-\phi) \frac{\nabla \phi}{|\nabla \phi|} \right] \quad (1)$$

where $\phi(x,t)$ is the level set function; x is the co-ordinate of system. If $\phi(x,t) > 0.5$, it refers to one phase; otherwise it refers to the other phase, Further, in the above equation, u is velocity (m/s); t is time (s); γ and ε are numerical stabilization parameters; ε is the thickness of the interface and has the same order of the mesh size; γ is the re-initialization parameter, and its value is the maximum value of u.

The Navier-Stokes (NS) equations and the continuity equation are the other two governing equations, and they are

$$\rho \left(\frac{\partial u}{\partial t} + u \cdot \nabla u \right) = \nabla \cdot [-pI + \eta(\nabla u + (\nabla u)^T)] + F_{st} \quad (2)$$

$$\nabla \cdot u = 0 \quad (3)$$

where ρ denotes density (kg/m3); η is the dynamic viscosity ($Pa \cdot s$); p is the pressure (Pa). $F_{st} = \sigma \kappa \delta n$ is the surface tension force (N/m3) acting on the interface between two phases, where σ is the surface tension coefficient; δ is the function concentrated at the interface between the two fluids; κ is the curvature of the interface which can be defined as $\kappa = -\nabla \cdot n$, where the normal vector n can be written as $n = \frac{\nabla \phi}{|\nabla \phi|}$.

The overall density ρ and viscosity η are calculated from:

$$\left.\begin{aligned} \rho &= \rho_1 + (\rho_2 - \rho_1)\phi \\ \eta &= \eta_1 + (\eta_2 - \eta_1)\phi \end{aligned}\right\} \quad (4)$$

where ρ_1, ρ_2, η_1 and η_2 are the densities and viscosities of fluid 1 and fluid 2, respectively.

B. Boundary and Initial Conditions

All the flows (middle-flow, sheath-flow, and cross-flow) were assumed to be laminar flows, as this droplet formation process was in micron scale. The pressure in the outlet was 0 Pa without viscous stress. The boundaries were in no-slip conditions. Q_s, Q_m, and Q_c are the flow rates of sheath-flow, middle-flow, and cross-flow, respectively. In this work, $Q_m = Q_s = 0.01$ ml/min were set to be constants. Fig. 3 illustrates the boundary and initial conditions. 9133 and 7815 triangular elements were applied for straight and crooked channel respectively considering accuracy and computational efficiency.

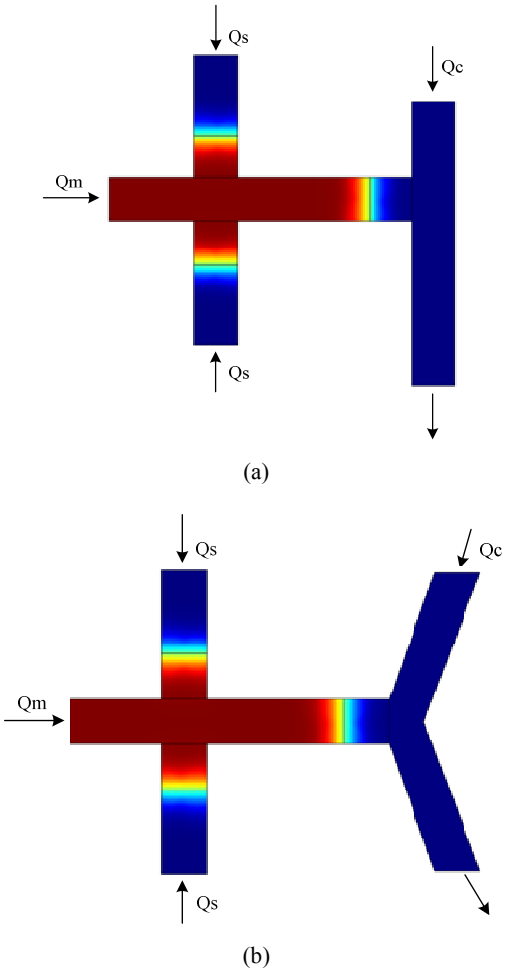

Fig. 3 Initial conditions for the simulation of the droplet formation process: (a) straight channel, (b) crooked channel

The numerical simulation was carried on using COMSOL Multi-physics 3.5 (COMSOL, Inc., Burlington, MA, USA) with the assumption of the two-dimensional and two-phase flow.

C. Experiments

Four devices were fabricated and tested in the experiment. Fig. 4 shows the experimental set-up. Three syringe pumps for sheath-flow, middle-flow and cross-flow were connected to the microchannel device controlling the flow rate of the fluids, an optical microscope was used to observe microsphere generation, and the images of microspheres were taken by a computer system connected to the microscope. A commercial image processing software was applied to measure the size of microspheres using the images Fig. 4 shows the experimental set-up.

TABLE III
DISTRIBUTION OF VELOCITY PROFILES FROM THE SIMULATION STUDY

1. m = 50 µm, straight channel, Q_c = 0.02 ml/min, PLGA concentration: 1%

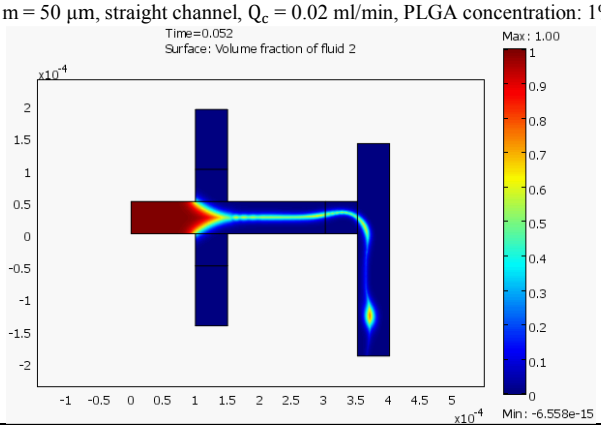

2. m = 75 µm, straight channel, Q_c = 0.03 ml/min, PLGA concentration: 15%

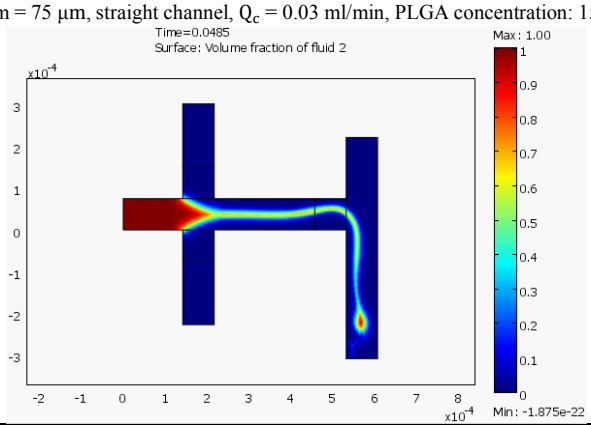

3. m = 50 µm, crooked channel, Q_c = 0.02 ml/min, PLGA concentration: 5%

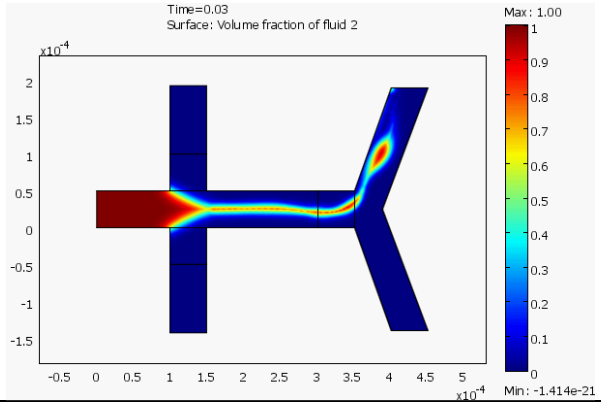

4. m = 100 µm, crooked channel, Q_c = 0.02 ml/min, PLGA concentration: 1%

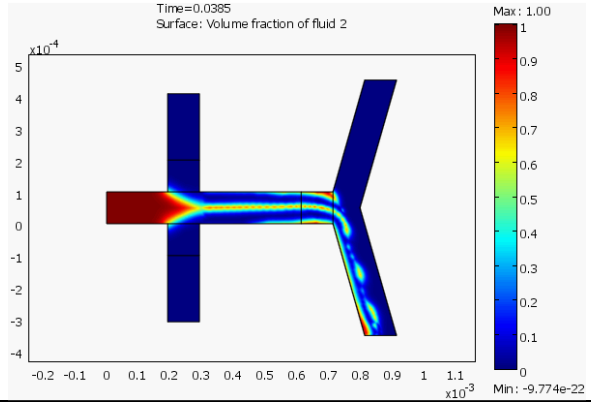

5. m = 50 µm, crooked channel, Q_c = 0.03 ml/min, PLGA concentration: 15%

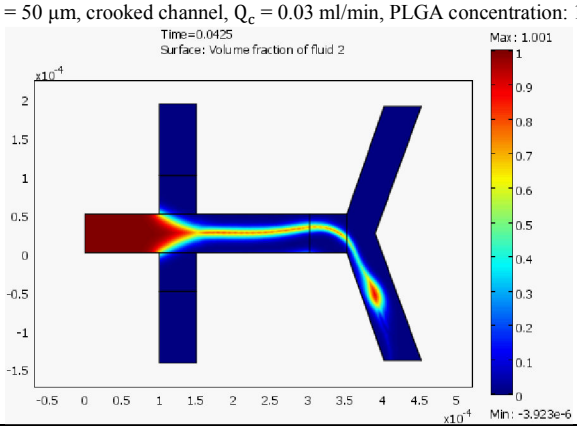

6. m = 100 µm, crooked channel, Q_c = 0.03 ml/min, PLGA concentration: 5%

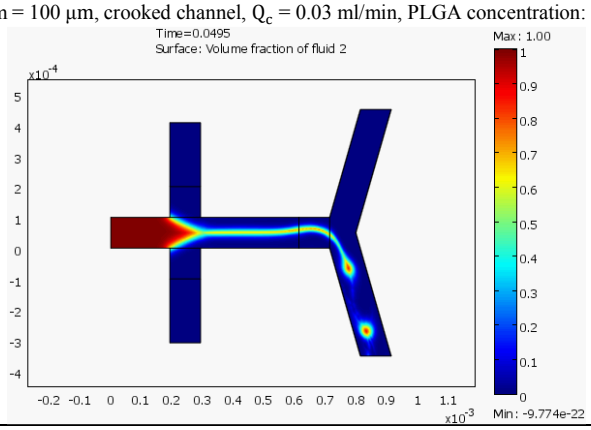

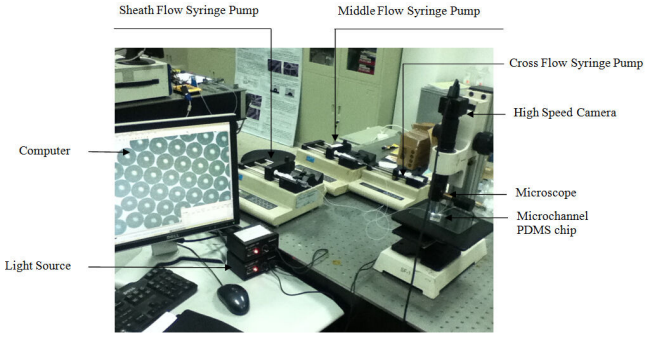

Fig. 4 Experimental set-up

V. Results with Discussion

Results of velocity distribution profiles are put in Table III.

Table IV and Fig. 5 conclude the numerical and experimental results of microsphere mean and standard (std) deviation of the sizes of microspheres. It is clear that the numerical and experimental results have a good agreement except for group 1, in which the calculated mean size of microsphere is twice the experimental one. This is probably caused by the unsteady environment during the experiments, or the channels in the devices might be clogged by PLGA after DCM has evaporated, leading to the dramatic disease of the size of the microspheres. Second, the structure of the device, channel size, PLGA concentration, and the cross-flow rate all may affect the microsphere size.

TABLE IV
Numerical and Experimental Results of Microsphere Mean Size

Experiment	Diameter of microspheres (μm)	
	Numerical	Experimental
1	21.33	10.98±1.81
2	41.57	39.42±4.73
3	23.18	21.04±2.21
4	49.05	47.98±4.72
5	45.81	43.15±3.22
6	33.95	35.56±3.83

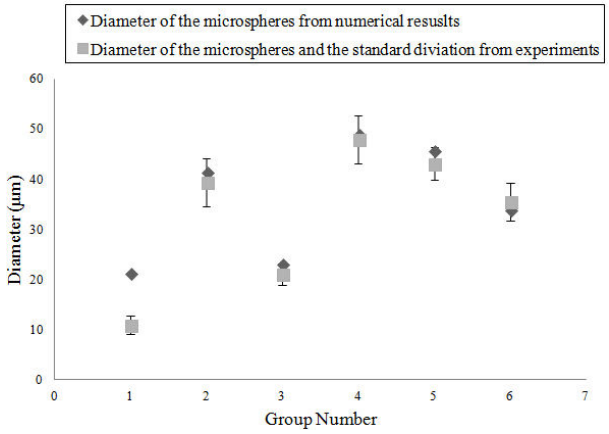

Fig. 5 Diameter of the microspheres from numerical and experimental results

Fig. 6 is an optical image of microspheres generated in the device with m = 50 μm, crooked channel, Q_c = 0.03 ml/min.

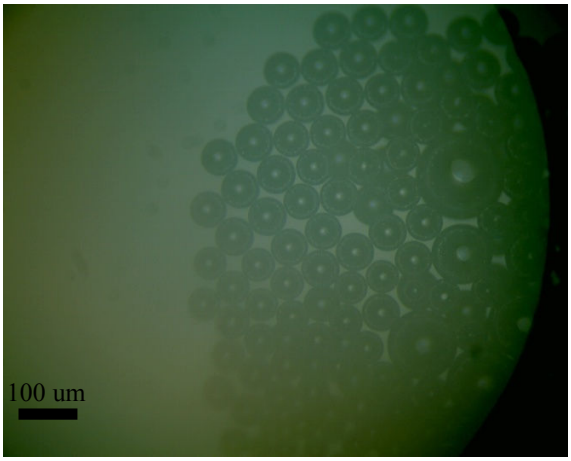

Fig. 6 Optical image of microspheres generated. m = 50 μm, crooked channel, Q_c = 0.03 ml/min

VI. Conclusion

The study presented in this paper was on the modeling of microspheres generation process in the context of the modified T-junction. Results obtained by this model were compared with experimental results. From the comparison, it can be concluded that a good agreement has been achieved. Thus the model is a reliable alternative of the measurement, which can be used to optimize the process parameters of the fluid and the device. Additionally, attentions need to be concentrated to the clog issue of the device in order to improve the accuracy and recyclability of the device.

Acknowledgment

The authors want to thank the financial support from SHRF (Saskatchewan Health Research Foundation) Phase I project grant to the corresponding author. The first and fourth authors would like to thank the financial support from China Scholarship Council.

References

[1] L. Amaya bower and T. Lee, "Lattice Boltzmann simulations of bubble formation in a microfluidic T-junction," *Philosophical Transactions of the Royal Society A: Mathematical, Physical and Engineering Sciences,* vol. 369, pp. 2405-2413, 2011.

[2] S. Arias, D. Legendre, and R. Gonzalez-Cinca, "Numerical simulation of bubble generation in a T-junction," *Computers & Fluids,* vol. 56, pp. 49-60, Mar 2012.

[3] N. C. Chen, J. Z. Wu, H. M. Jiang, and L. C. Dong, "CFD Simulation of Droplet Formation in a Wide-Type Microfluidic T-Junction," *Journal of Dispersion Science and Technology,* vol. 33, pp. 1635-1641, 2012.

[4] T. Glawdel and C. L. Ren, "Droplet formation in microfluidic T-junction generators operating in the transitional regime. III. Dynamic surfactant effects," *Physical Review E,* vol. 86, Aug 13 2012.

[5] X. Li, F. Li, J. Yang, H. Kinoshita, M. Oishi, and M. Oshima, "Study on the mechanism of droplet formation in T-junction microchannel," *Chemical Engineering Science,* vol. 69, pp. 340-351, Feb 13 2012.

[6] M. B. Mbanjwa, K. Land, L. L. Jewell, and I. M. Gledhill, "Experimental and numerical studies of emulsion formation in a microfluidic T-junction," presented at the AfriCOMP11: Second African Conference on Computational Mechanics, University of Cape Town, Cape Town, 2011.

[7] J. Sivasamy, T. N. Wong, N. T. Nguyen, and L. T. H. Kao, "An investigation on the mechanism of droplet formation in a microfluidic T-junction," *Microfluidics and Nanofluidics,* vol. 11, pp. 1-10, Jul 2011.

[8] K. Wang, Y. C. Lu, J. Tan, B. D. Yang, and G. S. Luo, "Generating gas/liquid/liquid three-phase microdispersed systems in double T-junctions microfluidic device," *Microfluidics and Nanofluidics,* vol. 8, pp. 813-821, Jun 2010.

[9] J. Wehking, M. Gabany, L. Chew, and R. Kumar, "Effects of viscosity, interfacial tension, and flow geometry on droplet formation in a microfluidic T-junction," *Microfluidics and Nanofluidics,* vol. 16, pp. 441-453, 2014/03/01 2014.

[10] S. Yeom and S. Y. Lee, "Size prediction of drops formed by dripping at a micro T-junction in liquid-liquid mixing," *Experimental Thermal and Fluid Science,* vol. 35, pp. 387-394, Feb 2011.

[11] R. F. Meyer, W. B. Rogers, M. T. McClendon, and J. C. Crocker, "Producing Monodisperse Drug-Loaded Polymer Microspheres via Cross-Flow Membrane Emulsification: The Effects of Polymers and Surfactants," *Langmuir,* vol. 26, pp. 14479-14487, Sep 2010.

[12] M. Pathak, "Numerical simulation of membrane emulsification: Effect of flow properties in the transition from dripping to jetting," *Journal of Membrane Science,* vol. 382, pp. 166-176, Oct 15 2011.

[13] R. D. Hancocks, F. Spyropoulos, and I. T. Norton, "Comparisons between membranes for use in cross flow membrane emulsification," *Journal of Food Engineering,* vol. 116, pp. 382-389, 2013.

[14] T. Schneider, G. H. Chapman, and U. O. Häfeli, "Effects of chemical and physical parameters in the generation of microspheres by hydrodynamic flow focusing," *Colloids and surfaces B: biointerfaces,* vol. 87, pp. 361-368, 2011.

[15] Q. J. Zhang, G. Y. Lin, Y. Wang, F. J. Yang, L. Ba, and D. G. Fu, "Formation of monodisperse cross-linked nanospherial condensates based on flow-focusing and droplet diffusion techniques," *Colloids and Surfaces a-Physicochemical and Engineering Aspects,* vol. 384, pp. 53-57, Jul 2011.

[16] K. Song, "Design and fabrication of novel microfluidic systems for microsphere generation," Doctor of Philosophy, Department of Biomedical Engineering, University of Saskatchewan, 2011.

[17] L. Lei, H. Zhang, D. J. Bergstrom, B. Zhang, and W. Zhang, "Modeling of droplet generation by a modified T-junction device using COMSOL," presented at the International Conference on Mechanical Design and Manufacturing, Hong Kong, 2014.

[18] K. Song and W. Zhang, "Design of a microchannel system using axiomatic design theory for size-controllable and monodispersed microspheres by enhanced perturbation," *The International Journal of Advanced Manufacturing Technology,* vol. 64, pp. 769-779, 2013.

[19] S. Osher and J. A. Sethian, "Fronts propagating with curvature-dependent speed-algorithms based on Hamilton-Jacobi formulations," *Journal of Computational Physics,* vol. 79, pp. 12-49, Nov 1988.